34th Annual International Conference of the IEEE EMBS
San Diego, California USA, 28 August - 1 September, 2012

Computer Assisted Detection of Liver Neoplasm (CADLN)

Shrinivas Bhosale[1], Ashish Aphale[2], Isaac Macwan[2],
Miad Faezipour[2], Priya Bhosale[4], and Prabir Patra[1,3*]
1 Department of Biomedical Engineering, University of Bridgeport
2 Department of Computer Science and Engineering, University of Bridgeport
3 Department of Mechanical Engineering, University of Bridgeport
4 Department of Diagnostic Radiology, M. D. Anderson Cancer Center, University of Texas

***Abstract* - To date, radiologists evaluate neoplasm images manually. Currently there is wide spread attention for developing image processing modules to detect and measure early stage neoplasm growth in liver. We report the fundamentals associated with the development of a multifunctional image processing algorithm useful to measure early growth of neoplasm and the volume of liver. Using CADLN, a radiologist will be able to compare computer generated volumetric data in serial imaging of the patients over time, that eventually will enable assessing progression or regression of neoplasm growth and help in treatment planning.**

I. Introduction

A. Background

In the United States more than 11 million people suffer from some form of cancer. Out of approximately 200 different types of cancer, many are quite rare forms.

Liver cancer is a deadly disease with surgical resection as the best treatment available, but may apply only when some conditions on tumor sizes are met. Therefore early diagnosis and accurate appraisal of tumors are critical.

In today's world the detection and diagnosis of liver neoplasm is based upon different imaging modalities such as Ultrasound, MRI (Magnetic Resonance Imaging), CT (Computed Tomography) and PET (Positron Emission Tomography) [1]. However, CT is ubiquitously available and preferred imaging modality among clinical practitioners. The detection of liver neoplasm in CT images is challenging due to the small observable changes between healthy tissues and tumoral ones [2].

B. Motivation and Contribution

We design and develop *Computer Assisted Detection of Liver Neoplasm* (CADLN) to increase the accuracy and efficiency of liver neoplasm detection and measurement. It has been reported that the cancer alone was responsible for the deaths of 600,000 patients worldwide in 2001 [3, 4]. Therefore, early diagnosis and accurate appraisal of tumors are critical.

A good method to detect the tumors is required to provide an added advantage to radiologist. CADLN may be efficient in detecting diverse tumor types, thereby, avoiding multiple and successive segmentations. The scanning technologies that exist today generate images ranging from 400 to 1500 per patient. It is cumbersome and time consuming for a radiologist to study each and every image. CADLN will help reduce the risk of liver surgery and design treatment strategies [5].

There is a need for advanced image processing tools to help radiologist come up to a decision much faster than what they can do today. CADLN will provide an aid to the doctors so that they can avoid unnecessary needle biopsy, with an added advantage of information and images provided by the CADLN to improve diagnosis [6]. Our algorithm is a blend of traditional as well as advanced digital imaging algorithms.

CADLN includes a feature amenable to case comparative study of the patient so that a radiologist can compare two image sets of the same patients over time.

In this case comparative study, we should be able to compare two sets of data of the same patient, and be able to asses change in tumor size and volume which may help in appropriate treatment planning of the patients.

II. Methodology and Procedure

CADLN consists of a number of steps described in this section. A flowchart of the CADLN procedure is provided in Figure 1.

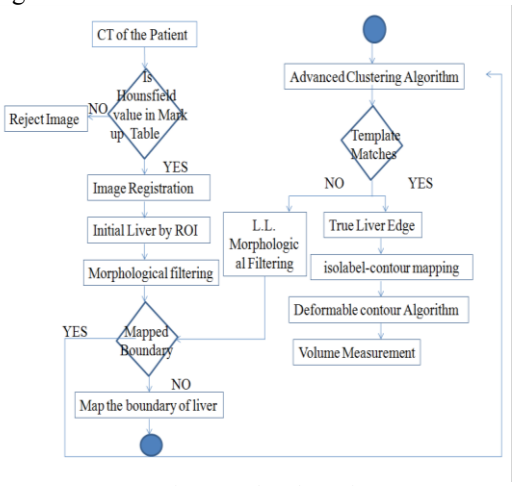

Figure 1. Flowchart of CADLN

A. Hounsfield Values

Hounsfield values are the numeric values contained in each pixel of a CT image. Hounsfield values represent the density of the tissue and are related to the composition and nature of the tissue imaged. The Hounsfield Unit (HU) equation is expressed as follows:

$$HU = [[\mu(X) - \mu (water)] \div \mu (water)] * 1000 \quad (1)$$

* Corresponding Author

Reference:- Uwe Schneider et al "The calibration of CT Hounsfield values for radiotherapy treatment planning " Phy. Med. Bio. 41 (1996) 111-124.

$\mu(X)$ is the average linear attenuation coefficient. $\mu(water)$ is linear attenuation coefficient of water (0).

In accordance with this system, lesions whose attenuation values are close to that of water are consistent with, but not specific for cysts. These are generally composed of fat as fat produces negative Hounsfield values. However, some types of soft tissues contain great amounts of fat, and some of the fat cells reveal abundant non-fatty tissues. Swollen blood characteristically demonstrates inhomogeneous areas with regions of both high attenuations (approximately 50 HU). Table I shows typical Hounsfield values for various tissues.

TABLE I. Hounsfield values of different tissues.

Tissue	Hounsfield Value
Liver	40 – 70
Grey matter	~37-45 HU
Blood	40
Fat	-50 - -100
Hepatic Vein	192-235

Table: - Markup Table

B. Image Registration

We divided the abdominal CT images to get a set of 12-20 image slices by Hounsfield value segmentation as discussed above. These images are then divided into non-overlapping blocks of 64 × 64 pixels. The partitioning of 64 x 64 pixels is performed on the images to analyze the liver boundary and liver muscles within the ROI.This inturn help in understanding the intensity distribution features from the liver. From CT images generated at M.D.Anderson Cancer center radiologists assign the liver position, that is labeled as ROI. There are several image slices that are manually segmented liver and adjacent muscle. Threshold value is varied in order to analyze the intensity of the liver ROI [7, 8]. The threshold values were manually varied to determine a specific set of threshold values where a clear liver boundary is identified (visible). This threshold value separates liver boundary from liver muscles.The Hounsfield values of the liver tissues in the ROI are compared with the Hounsfield values in the markup table.

This step is to understand if the image contains tumor and mark the slices with those that show tumoral Hounsfield values.

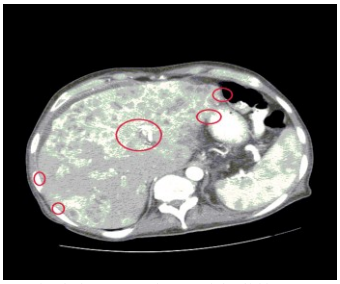

Figure 2. CT of Abdomen, Liver with different pattern structures (Courtesy, MD Anderson Cancer Center).

C. Initial Liver by Region of Interest (ROI)

The initial liver represents the preliminary outline of the liver In the ROI, the multilevel thresholding refers to using different threshold values from the set of threshold values initially computed to obtain a clear and prominent liver boundary. In doing so some we make the liver edge prominent leaving other unwanted section out. [7]

The liver boundary is found when a specific threshold value provides a consecutive edge to make liver boundary within the ROI. Preliminary Liver boundary within the ROI undergoes morphological filtering to obtain a clear smooth edges of the boundary for progressive and subsequent analysis. The CADLN based algorithm is designed to progressively perform operation to enhance the liver outline found in the first step to obtain the envelope of the liver in neighboring consecutive CT slices.

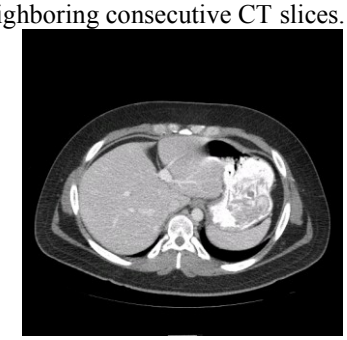

Figure 3. Liver with saddle like structures (Courtesy: MD Anderson Cancer Center)

D. Morphological Filtering

As image registration classifies each pixel into clustered liver class and scattered non-liver class, we perform mathematical morphology filtering to reduce scattered class and detect liver object.

$$(f \otimes Bn)(x,y) = \min\{f(x+l, y+m) \mid (l,m) \in Bn\}$$
$$(f \otimes kBn)(x,y) = \{\underbrace{(((f \otimes Bn) \otimes Bn) \otimes \ldots Bn}_{Ktimes})(x,y)\}$$
$$(f \oplus Bn)(x,y) = \max\{f(x-l, y-m) \mid (l,m) \in Bn\}$$
$$(f \oplus kBn)(x,y) = \{\underbrace{(((f \oplus Bn) \oplus Bn) \oplus \ldots Bn}_{Ktimes})(x,y)\}$$

(2)

In the above formulations, k is an integer representing the scale factor of structuring element (Se). Where theoretically, shape oriented approach is treated by the image as a set and the control of operation is another set, commonly known as structuring element (Se), B stores the threshold value for the shape. l and m represents the scaling value of x and y respectively. Whereas n represents the size of B. Multi scale filtering is performed by using the composition of the k-th order morphological erosion and dilation operations with the multi size Sf of the 5x5 and 3x3 flat size. The size of Se is decided by analyzing the number of remained regions or pixels of the threshold image, and k value is experimentally 4 or 5. The shape and size of the Se play important roles in detecting or extracting features of given shape and size from image [7, 9].

Morphological filtering is operated on the ROI blocks in threshold image. Seong-Jae Lim et al., 2003, recursively

performed morphological filtering based on region-labeling and clustering to get the first search region and the second search region. The final search range was decided by excluding the second search region from the first search region. [10, 11].

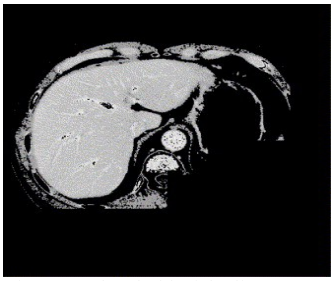

Figure 4. Threshold of the liver [7]

E. Mapped Boundary

The image obtained by varying threshold value (multilevel morphological filtering) reduces the noise level in the ROI thus preserves the shape of the liver, and detects the initial liver region [8].

The technique used for region finding is the breadth-first search approach. To reduce the noise and detect the coarse liver region, we use a 4-connected region-labeling algorithm. [12] After performing the region-labeling algorithm, the largest labeled region is marked as the region of the liver. If the boundary does not match the template then low level morphological filtering algorithm is applied to provide an accurate boundary and the process is repeated.

F. Clustering Algorithm

This is used to filter the adjoining non-liver organs and muscles that are still remained. In order to filter, we use region classifying by the modified *K*-means algorithm.

In this process, the region is divided into the adjacent noise of the liver and the liver region. Then, it is followed by reducing the class of the adjacent noise and getting the fine initial liver region. Finally, the image of the first search region is constructed by performing different order's composition between erosion and dilation operation of the mathematical morphological opening on the clustered initial liver region.

$$(f \circ iB_n)(x,y) = ((f \otimes iB_n) \oplus (i+j)B_n)(x,y) \quad (3)$$

In Equation (3) B is the scale factor of the Se. *i* and *j* are parameters that decide the size of the search range. Generally, *i* is 2 and *j* is 4 or 5 [1].

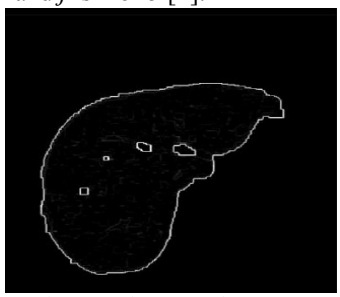

Figure 5. Liver Boundary [7]

G. Template Matching

A template is created for each specific patient with its liver boundary and the liver boundary is matched using an algorithm called "object matching of deformable object". We look for liver edge in all respective images that are separated at the initial level [13].

$$D_{\xi}(x,y) = \sum_{m=1}^{M}\sum_{n=1}^{N} \frac{\xi^{x}_{mn} \cdot e^{x}_{mn} + \xi^{y}_{mn} \cdot e^{y}_{mn}}{\lambda_{mn}} \quad (4)$$

In the above equation, D is the displacement of parameter vector ξ. Parameter $\xi = \{(\xi^{x}_{mn}, \xi^{y}_{mn})m, n=1,2,3\ldots\}$ and $\lambda_{mn} = \alpha\Pi^{2}(n^{2}+m^{2})$, where n, m=1,2,3.. This function preserves the connectedness of the liver boundary of the prototype template. The above equation also preserves the smoothness of the image while m and n are not too large.

If the template does not match, a low level morphological filtering is done on the image and the image is sent back to boundary mapping to confirm the liver boundary.

Figure 6. Liver with neoplasm (Courtesy: MD Anderson Cancer Center).

At this event, the liver boundary is matched and it is then sent out to true liver edge. Here, the liver edge is matched on the real image and those Hounsfield values within the true liver boundary are kept untouched while those not matching are left for the radiologist to rectify for a possible tumor. The images whose Hounsfield value matches to the tumor value are marked red as tumor, while those objects that show abrasive edges are marked problematic but needs confirmation from being called neoplasm.

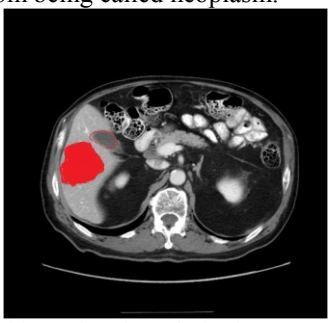

Figure 7. Liver with neoplasm is marked red (CADLN processed image - Hounsfield segmentation)

H. Countor Based Liver Segmentation

This algorithm is designed to deform the initial liver boundary within the search range to find clear and final liver contour. In order to get rid of saddle like patterns or

tortuous like structures, we classify the entire pattern into three cases. In the first case, the liver is adjacent to the air region which has low intensity value. The intensity gradient is monotonic in raw image; the pattern of labels in the isolable-contour map is monotonic as well. The dense contour patterns are in the areas of abrupt intensity gradients and widespread contour patterns lie in the areas of gradual intensity gradients [13].

The second is the case that liver is touched to the ribs or the kidney which has high intensity value. In the last case in which the liver is adjoined to the stomach or the lung, the intensity value within the liver boundary is distributed through the low gray level. We can get a correct liver contour by finding optimal path which is the minimal cost value. The local cost function combining three features is defined as:

$$l(p,q) = wD \cdot fD(p,q) + wB \cdot fB(q) + wIfI(q) \quad (5)$$

Each w is the weight of the corresponding feature function. Experimentally, weights of $wD = 0.3$, $wB = 0.3$, and $wI = 0.4$ seem to work well. The p and q values are two neighboring pixels in the gradient-label map, and $l(p,q)$ represents the local cost on the directed link from p to q [13].

I. Volume Calculation

We calculate the volume measurement of the liver by using thickness and interval information of the slice and size of the pixel. The following equation is used for volume measurement using the previous segmented liver region.

$$Volume = \sum_{i=1}^{N-1} \underbrace{((Lp * X * Y) + (Lp * X * Y))/2)}_{S_i} * \underbrace{}_{S_{i+1}} D \quad (6)$$

where N is the number of the slices including the segmented liver region, S_i is the slice number, D is the interval of the slice, Lp is the number of the pixel in the segmented liver region, and X,Y are the size of a pixel [15].

J. Results

The result is a set of images. The set contains liver with or without neoplasm. The each image in the set is the copy of the original with its respected liver boundary and all possible tumoral regions are marked with a red boundary for the radiological assessment. Mathematical data provided to the radiologist are the volumetric data of the areas in question such as liver and its neoplasm's.

Conclusion

This CADLN is introduced to assist the radiologist in detecting and measuring a tumor. The CADLN software will provide volumetric data of the tumor, thus helping in treatment planning. In the era of diagnostic imaging, CADLN will help save time for the radiologist by discarding redundant images. Moreover, a 3D view can provide an appropriate insight needed for surgical planning. Case comparative study enables radiologist to monitor the tumor in the efficient way possible.

Abbreviations

CADLN: - Computer Assisted Detection of Liver Neoplasm
CT: - Computed Tomography
ROI: - Region of Interest
HU: - Hounsfield Unit
LL: - Low Level

References

[1] M. Olivia et al., "Liver Cancer Imaging: Role of CT, MRI, US, and PET", in *Cancer Imagin , pp. S42-S46*, 2004.

[2] A Moghe et al., "Automatic Threshold Based Liver Lesion Segmentation in Abdominal 2D CT Images", in *International Journal of Image Processing (IJIP), Vol.5, no.* 2, *pp. 166-176*, 2011.

[3] A. Militzer et al., "Automatic Detection and Segmentation of Focal Liver Lesions in Contrast Enhanced CT Images", in *IEEE International Conference on Pattern Recognition , pp*. 1051-4651, 2010.

[4] "The World Health Report" World Health Organization. http://www.who.int/whr/en/

[5] Y. Hame, T. Alhonnoro and M. Pollari, " Image Analysis for Liver Tumor Ablation Treatment Planning," (*unpublished work*).

[6] E.-L. Chen, P.-C. Chung, C.-L. Chen, H.-M. Tsai and C.-I. Chang, "An Automatic Diagnostic System for CT Liver Image Classification" in *IEEE Transactions on Biomedical Engineering,Vol. ,5 no. 6*, *pp*. 783-794, June 1998.

[7] S.-J. Lim, Y.-Y. Jeong and Y.-S. Ho, "Automatic Liver Segmentation for Volume Measurement in CT Images", in *Journal of Visual Communication, Vol. 17, no. 4, pp. 860–875*, Aug. 2006.

[8] S. J. Lim, Y. Y. Jeong, C. W. Lee and Y. S. Ho, "Automatic Segmentation of the Liver in CT Images Using the Watershed Algorithm Based on Morphological Filtering, , in *Proc. SPIE 5370, pp. 1658–1666*, 2004.

[9] S. Mukhopadhayay et al., "Multiscale Morphological Segmentation of Grayscale Images," in *IEEE Transactions on Image Processing, Vol. 12, no. 5, pp. 533-549*, June 2003

[10] R.C. Gonzalez, R.E. Woods, "Digital Image Processing," *Prentice-Hall, Englewood Cliffs, NJ*, 2002.

[11] M.C. Kim, J.G. Choi, D.H. Kim, H. Lee, M.H. Lee, C.T. Ahn, and Y.S. Ho, "A VOP Generation Tool: Automatic Segmentation of Moving Objects in Image Sequences Based on Spatio-Temporal Information," in *IEEE Transactions in Circuits and Systems, Video Technology, vol. 9, no. 8, pp. 1216–1226*, 1999.

[12] E. Gose, R. Johnsonbaugh, S. Jost, Pattern Recognition and Image Analysis, Prentice-Hall, Englewood Cliffs, NJ, 1996A.

[13] Jain et al., "Object Matching Using Deformable Templates" in *IEEE Transaction on Pattern Analysis and Machine Intelligence*, *vol. 18, no. 3, pp. 267-278*, March 1996.

[14] E. N. Mortensen, W. A. Barrett, "Interactive Segmentation with Intelligent Scissors, in *Graphical Models and Image Processing, pp. 349-384*, 1998.

[15] H.Y. Kim, "Computer Based Automatic Segmentation and Volume Measurement of the Liver and Spleen in Contrast-Enhanced Helical CT Images," *A Thesis for the degree of Doctor of Philosophy of Medicine in Chungnam National University*, 2002.